Physical properties of $A_xFe_{2-y}S_2$ (A=K, Rb and Cs) single crystals

J. J. Ying, Z. J. Xiang, Z. Y. Li, Y. J. Yan, M. Zhang, A. F. Wang, X. G. Luo and X. H. Chen*
Hefei National Laboratory for Physical Science at Microscale and Department of Physics, University of Science and Technology of China, Hefei, Anhui 230026, People's Republic of China

We successfully synthesized two new compounds $Rb_xFe_{2-y}S_2$ and $Cs_xFe_{2-y}S_2$ which were isostructural with $K_xFe_{2-y}Se_2$ superconductor. We systematically investigated the resistivity, magnetism and thermoelectric power of $A_xFe_{2-y}S_2$ (A=K, Rb and Cs) single crystals. High temperature resistivity and magnetic measurements show anomalies above 500 K depending on A which are similar to $A_xFe_{2-y}Se_2$. Discrepancy between ZFC and FC curves was observed in $K_xFe_{2-y}S_2$ and $Rb_xFe_{2-y}S_2$, while it disappears in $Cs_xFe_{2-y}S_2$. Our results indicate the similar magnetism between $A_xFe_{2-y}S_2$ and $A_xFe_{2-y}Se_2$ at high temperature.

PACS numbers: 74.25.-q, 74.25.Ha, 75.30.-m

The discovery of iron-based high temperature superconductors attracted much attention in these years and it provided a new family of materials to explore the mechanism of high-T_c superconductivity besides cuprate superconductors[1–4]. Among all the iron-based superconductors, the anti-PbO type $FeSe_x$ owning the simplest structure with the edge-sharing $FeSe_4$ tetrahedra formed FeSe layers stacking along the c-axis. $FeSe_x$ displays a lower T_c of 8 K at ambient pressure[5] and T_c can reach 37 K (onset) under 4.5 GPa.[6] The corresponding pressure dependent ratio of T_c can reach as large as dT_c/dP of $\sim$ 9.1 K/GPa, which is the highest among all the Fe-base superconductors.[6–9]. Recently, by intercalating K, Rb, Cs and Tl between the FeSe layers, superconductivity has been enhanced to about 30 K without any external pressure in Fe-Se system[10–15]. The $A_xFe_{2-y}Se_2$ (A=K, Rb, Cs and Tl) superconductors are isostructural to 122 iron-pnictide superconductors. Unlike the iron-pnictide superconductors, large amount of A and Fe vacancies exist in the samples and it is amazing that superconductivity can still survive in the Fe layers. $A_xFe_{2-y}Se_2$ undergoes structural transition and antiferromagnetic transition around 500 K[19,20] which is much higher than that in iron-pnictide superconductors. The mechanism of superconductivity and its relationship with structural and antiferromagnetic transition in this system are still unknown. Superconductivity can be gradually suppressed through S doping[16,17]. For $K_xFe_{2-y}S_2$, it is a small gap semiconductor and shows spin-glass behavior below 32 K[18]. The fundamental differences between the superconducting samples $K_xFe_{2-y}Se_2$ and non-superconducting samples $K_xFe_{2-y}S_2$ is not clear and detailed physical properties of intercalated FeS samples need further investigation.

In this paper, we successfully synthesized two new compounds $Rb_xFe_{2-y}S_2$ and $Cs_xFe_{2-y}S_2$ which were isostructural to $K_xFe_{2-y}S_2$. We systematically investigated the physical properties of $A_xFe_{2-y}S_2$ (A=K, Rb and Cs) single crystals. Resistivity and magnetic measurements show anomalies above 500 K depending on A. We attribute these anomalies to the structural and antiferromagnetic transitions compared to the isostructural superconducting $A_xFe_{2-y}Se_2$ (A=K, Rb and Cs) compounds. $K_xFe_{2-y}S_2$ shows semiconductor behavior at low temperature the same to the previous report. The resistivity of $Rb_xFe_{2-y}S_2$ and $Cs_xFe_{2-y}S_2$ shows broad humps which is similar to superconducting $A_xFe_{2-y}Se_2$ samples, but no superconducting transition was observed in these samples. Single crystals of $A_xFe_2S_2$ were characterized by powder X-ray diffraction (XRD), X-ray single crystal diffraction, Energy-dispersive X-ray spectroscopy (EDX), direct current (dc) magnetic susceptibility, electrical transport and thermoelectric power(TEP) measurements. Resistivity below 400 K was measured using the Quantum Design PPMS-9. The resistivity measurement above 400 K was carried out with an alternative current resistance bridge (LR700P) by using the a Type-K Chromel-Alumel thermocouples as thermometer in a home-built vacuum resistance oven. Magnetic susceptibility was measured using the Quantum Design SQUID-MPMS. A high-temperature oven was used in the SQUID-MPMS for magnetic susceptibility measurement above 400 K.

Single crystals $A_xFe_{2-y}S_2$ were grown by Bridgeman method with the nominal composition A:Fe:S = 0.8:2:2. Starting material FeS was obtained by reacting Fe powder with S powder with Fe: S = 1: 1 at 700°C for 4 hours. Alkali metals and FeS powder were sealed into two wall quartz tubes. The mixture was heated to 1050 °C in 4 hours and then kept at this temperature for 2 hours, and later slowly cooled down to 750 °C at a rate of 6 °C/ hour. After that, the temperature was cooled down to room temperature by shutting down the furnace. Plate-like single crystals can be cleaved from the final products.

Figure 1 shows the X-ray single crystal diffraction and powder XRD after crushing the single crystals to powder for $A_xFe_{2-y}S_2$. Only ($00l$) diffraction peaks were

*Corresponding author; Electronic address: chenxh@ustc.edu.cn

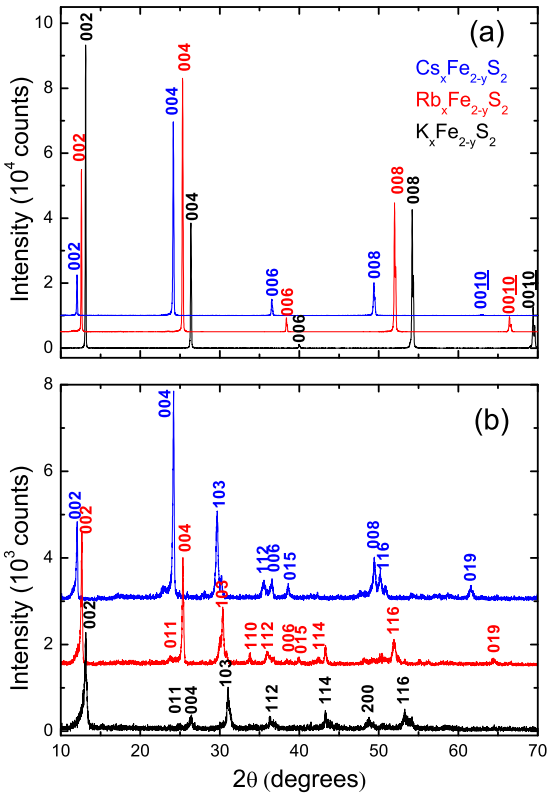

FIG. 1: (color online). (a) The single crystal x-ray diffraction pattern of $A_xFe_{2-y}S_2$, Only $(00l)$ diffraction peaks show up which indicating that the c axis is perpendicular to the plane of the plate. (b) X-ray diffraction pattern of the powdered $A_xFe_{2-y}S_2$.

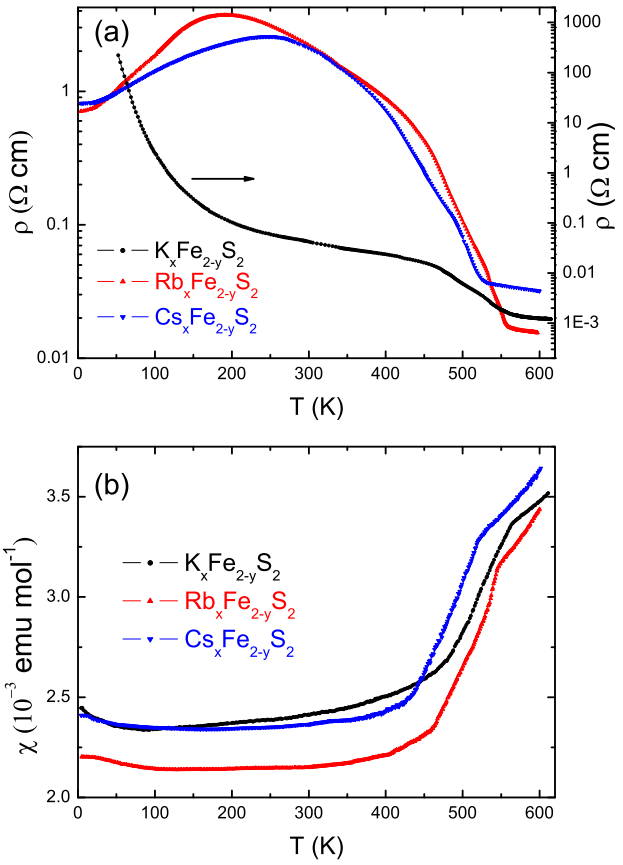

FIG. 2: (color online). (a) The temperature dependence of the resistivity for $A_xFe_{2-y}S_2$. (b) The temperature dependence of the magnetic susceptibility with field of 5 T applied along the ab plane for $A_xFe_{2-y}S_2$.

observed, suggesting that the crystallographic c axis is perpendicular to the plane of the single crystal. The lattice constants of c-axis for $K_xFe_{2-y}S_2$, $Rb_xFe_{2-y}S_2$ and $Cs_xFe_{2-y}S_2$ were determined to be 13.546 Å, 14.070 Å and 14.801 Å respectively, it is consistent with the increasing of alkali ion radius from K to Cs. The lattice constants of a-axis for $K_xFe_{2-y}S_2$, $Rb_xFe_{2-y}S_2$ and $Cs_xFe_{2-y}S_2$ were determined to be 3.772 Å, 3.789 Å and 3.824 Å respectively. The actual compositions of $K_xFe_{2-y}S_2$, $Rb_xFe_{2-y}S_2$, $Cs_xFe_{2-y}S_2$ were determined by EDX to be $K_{0.68}Fe_{1.70}S_2$, $Rb_{0.74}Fe_{1.67}S_2$ and $Cs_{0.72}Fe_{1.71}S_2$ respectively.

Figure 2(a) shows the temperature dependence of the resistivity in the temperature ranges from 4 K to 620 K for $A_xFe_{2-y}S_2$. $K_xFe_{2-y}S_2$ shows semiconductor behavior at low temperature, being similar to the previous reports[16,17]. The resistivity of $Rb_xFe_{2-y}S_2$ and $Cs_xFe_{2-y}S_2$ shows broad humps which are similar to superconducting samples $A_xFe_{2-y}Se_2$[21,22], however no superconducting transition was observed at low temperature. The hump temperatures T_{hump} for $Rb_xFe_{2-y}S_2$ and $Cs_xFe_{2-y}S_2$ are 180 K and 250 K respectively. Sharp decrease in resistivity can be observed above 500 K for all the samples with increasing the temperature. The anomalies of resistivity for all the samples clearly indicate phase transition in this kind of materials above 500 K. In order to deep investigate this phase transition, we take magnetic measurement with the temperature up to 610 K. Fig. 2(b) shows the temperature dependence of magnetic susceptibility with the field magnitude of 5 T applied within ab plane for $A_xFe_{2-y}S_2$. The magnetic susceptibilities show sharp drop above 500 K with decreasing the temperature for all the samples which indicates antiferromagnetic transition at high temperature in this kind of materials. At the temperature below 400 K, the susceptibilities nearly show no temperature dependence.

We compared the high temperature resistivity with the susceptibility above 400 K as shown in Fig. 3. We found the anomaly temperature determined by the resistivity (T_r) is slightly higher than the antiferromagnetic transition temperature (T_N). The detailed temperatures of T_r and T_N for $A_xFe_{2-y}S_2$ are listed in Table

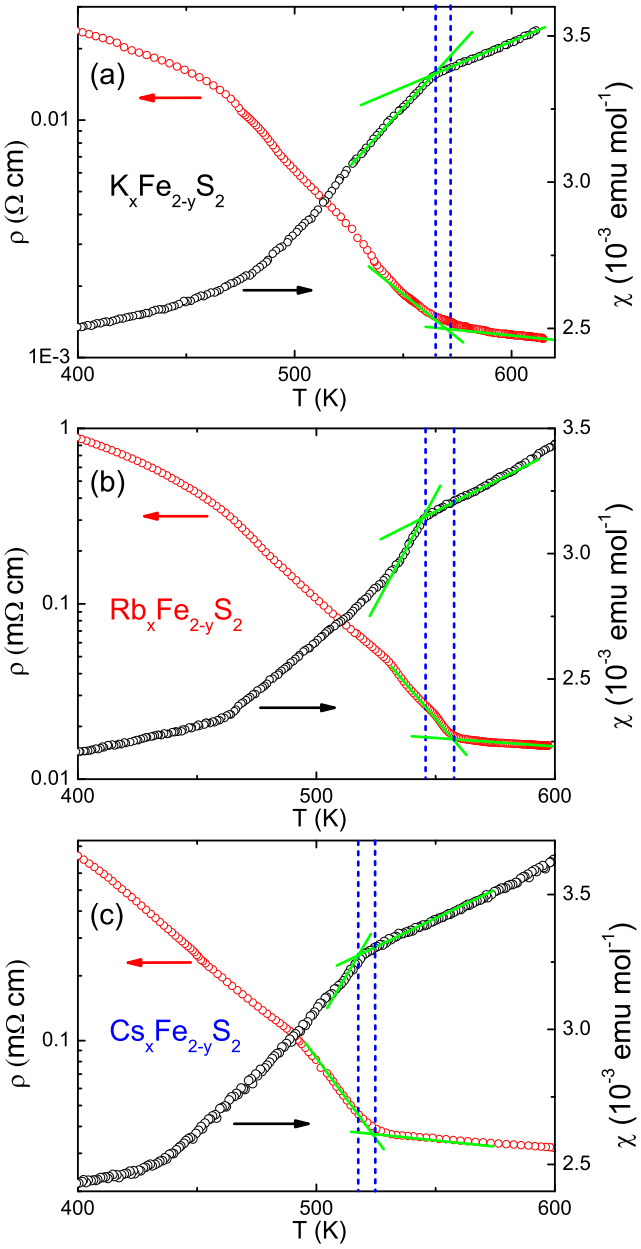

FIG. 3: (color online). The temperature dependence of resistivity and susceptibility around the temperature of T_N for $K_xFe_{2-y}Se_2$ (a), $Rb_xFe_{2-y}Se_2$ (b) and $Cs_xFe_{2-y}Se_2$ (c).

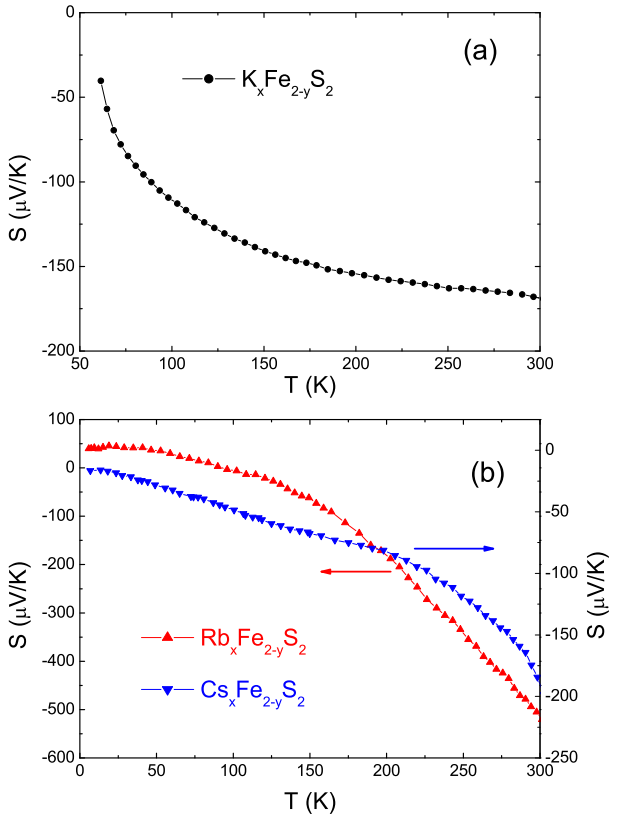

FIG. 4: (color online). The temperature dependence of thermoelectric power of $K_xFe_{2-y}S_2$ (a), $Rb_xFe_{2-y}S_2$ and $Cs_xFe_{2-y}S_2$ (b).

I. T_r and T_N increase with decreasing the lattice constant of c-axis. The temperature dependence of resistivity and susceptibility of $A_xFe_{2-y}S_2$ is very similar to its isostructural $A_xFe_{2-y}Se_2$ superconducting samples. T_r and T_N in $A_xFe_{2-y}S_2$ are about 20 K higher than those in $A_xFe_{2-y}Se_2$[20]. The structures between $A_xFe_{2-y}S_2$ and $A_xFe_{2-y}Se_2$ are the same and similar Fe vacancy ordering was observed in $K_xFe_{2-y}S_2$[17]. Considering the similarities of the structure and physical properties between $A_xFe_{2-y}S_2$ and $A_xFe_{2-y}Se_2$, we ascribe the sudden increase of resistivity to the structural transition arising from the Fe vacancy ordering. We can conclude that all the samples of $A_xFe_{2-y}Ch_2$(A=K, Rb and Cs, Ch=S,Se) exhibit the common features of antiferromagnetic and structural transition at high temperature. Although $A_xFe_{2-y}S_2$ and $A_xFe_{2-y}Se_2$ show the same physical properties in normal state, no superconductivity was found in $A_xFe_{2-y}S_2$.

Figure 4(a) shows the temperature dependence of TEP for $K_xFe_{2-y}S_2$. The TEP for $K_xFe_{2-y}S_2$ exhibits large negative value at room temperature. With decreasing the temperature, the absolute value of TEP gradually decreases and became small negative value at low temperature which is similar to $K_xFe_{2-y}Se_{2-y}S_y$[23]. Fig. 4(b) shows the temperature dependence of TEP for $Rb_xFe_{2-y}S_2$ and $Cs_xFe_{2-y}S_2$. The TEP for both the two samples shows negative value at room temperature. With decreasing the temperature, the absolute value of TEP for $Rb_xFe_{2-y}S_2$ gradually decreases and TEP shows small positive value at low temperature which indicates the multiple-band electronic structure in $Rb_xFe_{2-y}S_2$. For $Cs_xFe_{2-y}S_2$, the absolute value of TEP decreases with decreasing the temperature and still exhibit negative at low temperature. The different temperature de-

TABLE I: The summary of the actual compositions determined by EDX analysis with errors within 5%, the a-axis lattice parameters and the c-axis lattice parameters, the abnormal temperature determined by the susceptibility (T_N) and resistivity (T_r) for all the crystals $A_xFe_{2-y}S_2$ (A = K, Rb, Cs).

sample name	A: Fe: Se	a (Å)	c (Å)	T_N (K)	T_r (K)
$K_xFe_{2-y}S_2$	0.68: 1.70: 2	3.772	13.546	565	571
$Rb_xFe_{2-y}S_2$	0.74: 1.67: 2	3.789	14.070	546	558
$Cs_xFe_{2-y}S_2$	0.72: 1.71: 2	3.824	14.801	518	524

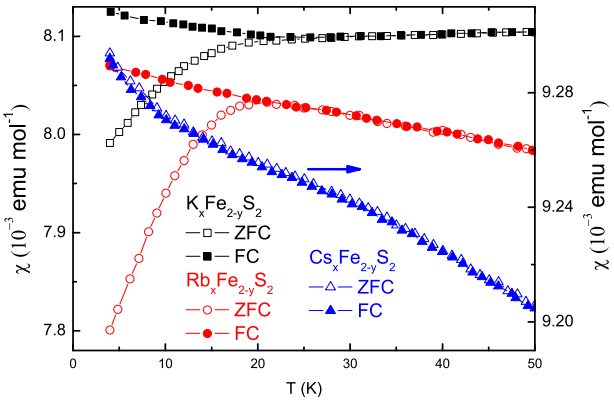

FIG. 5: (color online). ZFC and FC dc magnetic susceptibility with the field 1000 Oe applied within the ab plane for $A_xFe_{2-y}S_2$ at low temperature.

pendence of TEP for these samples might be due to the different doping contents which was caused by the different A and Fe content in the samples.

Fig.5 shows ZFC and FC dc magnetic susceptibility with the field 1000 Oe applied within the ab plane for $A_xFe_{2-y}S_2$ at low temperature. Obvious discrepancy between ZFC and FC curves was found for $K_xFe_{2-y}S_2$ and $Rb_xFe_{2-y}S_2$ below 20 K. Such behavior is not yet understood. However, discrepancy between ZFC and FC curves was not observed in $Cs_xFe_{2-y}S_2$.

The physical properties of $A_xFe_{2-y}S_2$ are very similar to its isostructural compounds $A_xFe_{2-y}Se_2$ except for the absence of superconductivity. The absence of superconductivity in $A_xFe_{2-y}S_2$ might be closely related to the structure and the content of A and Fe[17], however, it is still an open question and other experiment need to elucidate this problem. The superconductivity can be gradually suppressed through S substitution for Se in $K_xFe_{2-y}Se_2$[17]. However, the antiferromagnetic transition at high temperature stays the same which indicates the local magnetic exchange interactions between $A_xFe_{2-y}S_2$ and $A_xFe_{2-y}Se_2$ are almost the same. The transition temperatures for $A_xFe_{2-y}Ch_2$ slightly increase with the c-axis lattice parameters decreasing. The antiferromagnetic transition seems not directly connected to the superconductivity in this system. Almost the same antiferromagnetic transition temperatures between superconducting samples and insulting samples of $K_xFe_{2-y}Se_2$ samples also prove this[24]. The different resistivity behaviors at low temperature for these samples might be due to the phase separation in this system which is similar to $K_xFe_{2-y}Se_2$ samples[25]. The metallic phase without superconductivity may coexists with the insulating phase in this system, so with the different composition of metallic phase and insulating phase may results in the different hump temperatures. The maximum resistivity of $Rb_xFe_{2-y}S_2$ and $Cs_xFe_{2-y}S_2$ is about one order larger than the normal state resistivity of superconducting $A_xFe_{2-y}Se_2$[13], even in $K_xFe_{2-y}S_2$ no metallic resistivity behavior was observed. It indicates that the proportion of metallic phase in $A_xFe_{2-y}S_2$ is smaller than that in $A_xFe_{2-y}Se_2$. TEP clearly indicate the multi-band electronic structure in this system and the electronic structure is strongly dependent on A and Fe content in the samples. Discrepancy between ZFC and FC curves at low temperature might be related to the A and Fe content, or to the different Fe arrangement. The origin for the appearance of such behavior in this system still needs to be investigated.

In conclusion, we had successfully synthesized two new compounds $Rb_xFe_{2-y}S_2$ and $Cs_xFe_{2-y}S_2$ which were isostructural with $K_xFe_{2-y}S_2$. Resistivity and susceptibility anomalies were observed above 500 K for $A_xFe_{2-y}S_2$ single crystals which was similar to superconducting $A_xFe_{2-y}Se_2$ samples. TEP indicated the multi-band electronic structure which was common in iron-based superconductors. Discrepancy between ZFC and FC curves at low temperature was possibly related to the A and Fe content, or to the local environment of Fe ions[17].

ACKNOWLEDGEMENT This work is supported by the National Basic Research Program of China (973 Program, Grant No. 2012CB922002 and No. 2011CB00101), National Natural Science Foundation of China (Grant No. 11190020 and No. 51021091), the Ministry of Science and Technology of China, and Chinese Academy of Sciences.

[1] Y. Kamihara, T. Watanabe, M. Hirano, and H. Hosono, *J. Am. Chem. Soc.* **130**, 3296(2008).

[2] X. H. Chen, T. Wu, G. Wu, R. H. Liu, H. Chen and D. F. Fang, Nature **453**, 761(2008).

[3] Z. A. Ren, G. C. Che, X. L. Dong, J. Yang, W. Lu, W. Yi, X. L. Shen, Z. C. Li, L. L. Sun, F. Zhou and Z. X. Zhao, EPL **83**, 17002(2008).

[4] M. Rotter, M. Tegel, D. Johrendt, Phys. Rev. Lett. **101**, 107006(2008).

[5] F. C. Hsu, J. Y. Luo, K. W. The, T. K. Chen, T. W. Huang, P. M. Wu, Y. C. Lee, Y. L. Huang, Y. Y. Chu, D. C. Yan and M. K. Wu, Proc. Nat. Acad. Sci. **105**, 14262 (2008).

[6] S. Medvedev, T. M. McQueen, I. Trojan, T. Palasyuk, M. I. Eremets, R. J. Cava, S. Naghavi, F. Casper, V. Ksenofontov, G. Wortmann and C. Felser, Nat. Mater. **8** 630(2009)

[7] Yoshikazu Mizuguchi, Fumiaki Tomioka, Shunsuke Tsuda, Takahide Yamaguchi, and Yoshihiko Takano, Appl. Phy. Lett. 93, 152505 (2008)

[8] S. Margadonna, Y. Takabayashi, Y. Ohishi, Y. Mizuguchi, Y. Takano, T. Kagayama, T. Nakagawa, M. Takata, and K. Prassides, Phys. Rev. B 80, 064506 (2009).

[9] G. Garbarino, A. Sow, P. Lejay, A. Sulpice, P. Toulemonde, M. Mezouar, and M. Nunez-Regueiro, EPL **86** (2009).

[10] J. Guo, S. Jin, G. Wang, S. Wang, K. Zhu, T. Zhou, M. He and X. Chen, Phys. Rev. B **82**, 180520(R) (2010).

[11] Yoshikazu Mizuguchi, Hiroyuki Takeya, Yasuna Kawasaki, Toshinori Ozaki, Shunsuke Tsuda, Takahide Yamaguchi and Yoshihiko Takano, Appl. Phys. Lett. 98, 042511 (2011).

[12] A. F. Wang, J. J. Ying, Y. J. Yan, R. H. Liu, X. G. Luo, Z. Y. Li, X. F. Wang, M. Zhang, G. J. Ye, P. Cheng, Z. J. Xiang, X. H. Chen, Phys. Rev. B **83**, 060512(R) (2011).

[13] J. J. Ying, X. F. Wang, X. G. Luo, A. F. Wang, M. Zhang, Y. J. Yan, Z. J. Xiang, R. H. Liu, P. Cheng, G. J. Ye, X. H. Chen , Phys. Rev. B **83**, 212502 (2011).

[14] A. Krzton-Maziopa, Z. Shermadini, E. Pomjakushina, V. Pomjakushin, M. Bendele, A. Amato, R. Khasanov, H. Luetkens and K. Conder, J. Phys.: Condens. Matter **23**, 052203 (2011).

[15] Minghu Fang, Hangdong Wang, Chiheng Dong, Zujuan Li, Chunmu Feng, Jian Chen, H.Q. Yuan, EPL, **94**, 27009 (2011).

[16] Jiangang Guo, Xiaolong Chen, Gang Wang, Tingting Zhou, Xiaofang Lai, Shifeng Jin, Shunchong Wang, Kaixing Zhu, arXiv:1102.3505 (unpublished).

[17] Hechang Lei, Milinda Abeykoon, Emil S. Bozin, Kefeng Wang, J. B. Warren, C. Petrovic, Phys. Rev. Lett. **107**, 137002 (2011).

[18] Hechang Lei, Milinda Abeykoon, Emil S. Bozin, and C. Petrovic, Phys. Rev. B **83**, 180503(R) (2011).

[19] Wei Bao, Q. Huang, G. F. Chen, M. A. Green, D. M. Wang, J. B. He, X. Q. Wang, and Y. Qiu, Chi. Phys. Lett. **28**, 086104 (2011)

[20] R. H. Liu, X. G. Luo, M. Zhang, A. F. Wang, J. J. Ying, X. F. Wang, Y. J. Yan, Z. J. Xiang, P. Cheng, G. J. Ye, Z. Y. Li, X. H. Chen EPL, **94**, 27008 (2011).

[21] X. G. Luo, X. F. Wang, J. J. Ying, Y. J. Yan, Z. Y. Li, M. Zhang, A. F. Wang, P. Cheng, Z. J. Xiang, G. J. Ye, R. H. Liu, X. H. Chen, New J. Phys. **13**, 053011 (2011).

[22] J. J. Ying, X. F. Wang, X. G. Luo, Z. Y. Li, Y. J. Yan, M. Zhang, A. F. Wang, P. Cheng, G. J. Ye, Z. J. Xiang, R. H. Liu, X. H. Chen, New J. Phys. **13**, 033008 (2011).

[23] Kefeng Wang, Hechang Lei, and C. Petrovic, Phys. Rev. B **84**, 054526 (2011).

[24] Y. J. Yan, M. Zhang, A. F. Wang, J. J. Ying, Z. Y. Li, W. Qin, X. G. Luo, J. Q. Li, Jiangping Hu, X. H. Chen, arXiv:1104.4941 (unpublished).

[25] F. Chen, M. Xu, Q. Q. Ge, Y. Zhang, Z. R. Ye, L. X. Yang, Juan Jiang, B. P. Xie, R. C. Che, M. Zhang, A. F. Wang, X. H. Chen, D. W. Shen, X. M. Xie, M. H. Jiang, J. P. Hu, and D. L. Feng, arXiv:1106.3026 (unpublished).